Predictive Current Control Strategy Using ANFIS &LMS Algorithm for Control of PMSM Drive Systems

B.Bhagyamma[1], Dr.P.Sujatha[2]

[1] *PG scholar, department of EEE,JNTU Anantapuramu, Andhra Pradesh, India.*

[2] *Professor, department of EEE, JNTU Anantapuramu, Andhra Pradesh, India.*

---***---

Abstract – The description and analysis of PMSM is done based on its applications in Mechatronics. In industrial and robotic applications PMSM is used because of its characteristics like, high torque to volume ratio, low inertia and high and high efficiency. A closed loop control system with a Adaptive nuero Fuzzy Interface System(ANFIS) Plus Least Mean Square Algorithm (LMSA) controller is designed to operate in the speed loop of closed loop control system with flux weakening regions and constant torque angle. The design of simulink model based on field oriented control of PMSM drive has been implemented. All realistic components included in the drive such as current controller, speed controller, inverter and the motor. The variations in current, torque and frequency are analyzed during different speed control steps. Simulation results for both ANFIS and LMSA control schemes associated with current controllers are given for two speeds of operation, one above rated speed and at the rated speed.

Index Terms – Drive Systems, direct speed control (DSC), Adaptive nuero Fuzzy Interface System (ANFIS), Least Mean Square Algorithm (LMSA), permanent magnet synchronous machine (PMSM).

I. INTRODUCTION

The PMSM drives have been mostly applied in a wide variety of industrial applications [1-2]. This is due to the advantages of PMSM such as high power density and efficiency, high torque to inertia ratio and has high reliability. Now a days a continuous cost reduction of magnetic materials having high energy density and coercitivity doing the AC drives based on PMSM more attractive and competitive. In the best performance applications, the PMSM drives are ready to achieve sufficient requirements as fast dynamic response, good power factor and huge operating speed range. Due to this, a continuous increase in the use of PMSM drives will be surely founded in future [3-5].

This is also broadly applied in so many areas having servo like high performances plays a secondary role to reliability and energy savings. In order to get field oriented control of PMSM. The knowledge of the rotor position must be required. As the rotor position is going to be measured by shaft encoder, resolver or hall sensors

In case of "direct drive applications" PM machines are more advantageous for the vehicles as hybrid electrical vehicles (EHV) or electrical vehicles and washing machines [6]. By this technology, the rotating working unit of a direct drive is coupled to the motor shaft without transmission assembly, which may include different equipment. Such as gears, clutches, belts, pulleys and gearboxes. The motor delivers power directly to the working unit. The concept of direct drive system enables the high dynamic response, low acoustic noise, increased efficiency and long life time due to the elimination of the transmission component. At low speeds and at standstill the direct drive systems require large shaft torque as well as constant output power over a wide range of speed. The PM machines at low speed or below base speed are designed to operate not only constant torque mode but also in the constant power mode when above base speed.

The cost and size of the overall drive system can be reduced by this way. By the conventional vector control the constant torque operation of PM motor can be easily achieved. The back EMF of motor is larger than the line voltage when the speed is above the base speed. In that situation motor suffers from the difficulty to produce torque continuously due to voltage and current constraints [7]. For that the flux can be extended by applying negative magnetizing current component to weaken the air gap flux transform are used in wide range.

This paper is organized as follows. The plant is analyzed and shown in Section II, where also the main control goals are defined. In Section III, ANFIS&LMSA-DSC is synthesized and the required techniques are shown: past input compensation, state prediction, disturbance handling, state limitations, and the plant input selection via cost function. Furthermore, ANFIS&LMSA-DSC is tested and the results are shown in Section IV. The overall

control behaviour is evaluated such as the control offset suppression, the dynamic and steady-state behaviour.

II. ANASYSIS

A. Plant

The continuous time, permanent magnet synchronous machine (PMSM) model, which works with isotropic (or surface) and anisotropic (or interior) PMSM, is in the dq reference frame

$$I'_d = \frac{-R}{L_d} i_d + \frac{L_q \omega}{L_d} i_q + \frac{1}{L_d} u_d$$
$$I'_q = \frac{-R}{L_q} - \frac{L_d}{L_q} \omega i_d + \frac{1}{L_q} u_q - \frac{\lambda}{L_q}$$
$$T_e = \frac{3}{4} P(\lambda i_q + (L_d - L_q) i_d i_q) \qquad (1)$$
$$\dot{\omega} = -\frac{B}{J} + \frac{p}{J} T_e - \frac{p}{J} T_l$$

The model can be rewritten indiscrete time. The electrical state-space model is

$$x_e(k+1) = A_e x_e(k) + B_e u_e(k) + E_e$$
$$y_e(k) = C_e x_e(k) \qquad (2)$$

Where $x_e = y_e = \begin{bmatrix} i_d \\ i_q \end{bmatrix}$; $u_e = \begin{bmatrix} u_d \\ u_q \end{bmatrix}$, and

$$A_e = \begin{bmatrix} 1 - \frac{RT_s}{L_d} & \frac{L_q T_s}{L_d} \omega \\ -\frac{L_d T_s}{L_q} \omega & 1 - \frac{RT_s}{L_q} \end{bmatrix};$$

$$B_e = \begin{bmatrix} \frac{T_s}{L_d} & 0 \\ 0 & \frac{T_s}{L_q} \end{bmatrix}; \quad E_e = \begin{bmatrix} 0 \\ \frac{\lambda T_s}{L_q} \end{bmatrix};$$

$$C_e = \begin{bmatrix} 1 & 0 \\ 0 & 1 \end{bmatrix};$$

The matrices A_e and E_e depend on w, which requires their update during the execution of MP-DSC. The electrical torque can be calculated depending on $x_e(k)$

$$T_e(k) = \frac{3}{2} p(\lambda i_q(k) + (L_d - L_q) i_d(k) i_q(k) \quad (3)$$

The discrete mechanical state-space model is

$$x_m(k+1) = A_m x_m(k) + B_m u_m(k) + E_m \omega_m(k)$$
$$y_m(k) = C_m x_m(k) \qquad (4)$$

Where $x_m = \omega$, $u_m = T_e$, $\omega_m = T_l$, and

$$A_m = 1 - \frac{BT_s}{J} \quad , B_m = \frac{pT_s}{J},$$

$$E_m = -\frac{pT_s}{J}, C_m = 1$$

The motor accepts a finite set of voltages U_e from the voltage source inverter (VSI), i.e., $u_e(k) \epsilon U_e C R^{m_e}$ (further called input). Thus, $x_e(k) \epsilon X_e C \ R^{n_e}$ and $x_m(k) \epsilon X_m C R^{n_m}$ are the possible electrical and mechanical states respectively. Thus, by knowing the previous inputs and states of the system future of the states can be computed.

From this we can observe $u_e(k)$ is the plant input, which is generated by the VSI. $u_m(k)$ Is a consequence of the state $x_e(k)$. Thus, the input $u_e(k)$ leads to $x_e(k+1)$ and $x_m(k+2)$ taking into account the previous values, but $x_m(k+1)$ is independent of $u_e(k)$ and depends on $u_e(k-1)$. For the convenience in the evaluation of input, the values must be used which are dependent on the same input.

Moreover, the execution of a control algorithm takes a certain time $T_x > 0$. Thus, a practical implementation relies on measurements which are obtained previously, e.g., $y_e(k-1)$ and $y_m(k-1)$. For high performance control, the state variation between measurement and actuation instant should be compensated.

B. Control

(1) Besides practical asymptotic stability [17], the minimum requirements on a controller of a discrete time system is, , the tracking of a reference signal, i.e., $\lim_{t \to +\infty} \| x - x^* \| < \epsilon$, where is small. In the case of a speed controller. i.e., MP-DSC, the goal is $\lim_{t \to +\infty} \| x_m - x_m^* \| < \epsilon$, .

(2) takes implicitly input limits into account but the states must be limited to their rated values $x(k) \le x_r$, where $x_r \in R^n$. Moreover, a plant has limits for the states and inputs. In this paper, the x_m is assumed to be limited externally by limiting the reference value. On the other hand, the electrical states, i.e., the current amplitude must be limited to the maximum admissible value, i.e., $\| x_e \| \le I_r$.
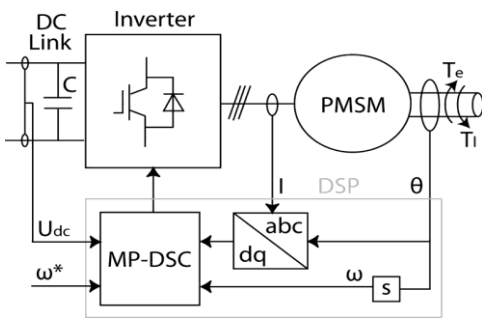
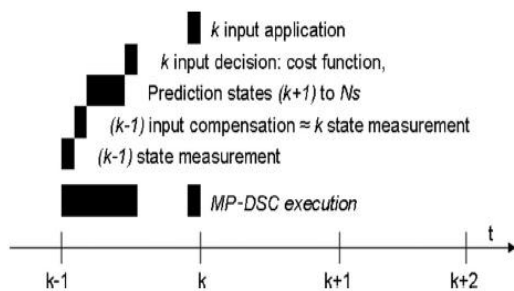**Figure 1: PMSM-VSI drive system with MPC**

Figure 2: Execution of the MP-DSC algorithm

On the control algorithm additional demands may arise. Such as, high current quality leads to as small torque ripple, or the machine should work close to the maximum torque per ampere (MPTA) trajectory in order to obtain a high steady state, i.e., equilibrium condition efficiency. If over-speed capabilities are desired, the controller must work off the MTPA trajectory in order to weaken the stator flux.

III. ANFIS&LMSA-DSC

Here, the execution of the ANFIS&LMSA-DSC algorithm is shown. Measurement, prediction, input selection, and actuation are the main four parts in the operation [9]. In period of (K-1) the necessary states are measured and delays are compensated and disturbances are rejected for the period (K+1)………N states future plant states are to be computed. By using cost function and with lowest cost input the results are evaluated in the period of K. Figure 2 shows MP-DSC execution.

As shown in figure 3 integral part of adaptive beam forming system forms uniform linear array with N isotropic elements. The antenna array give the output x(t) as

$$x(t) = s(t)a(\theta_0) + \sum_{i=1}^{N_u} u_i(t)a(\theta_i) + n(t) \ldots.(5)$$
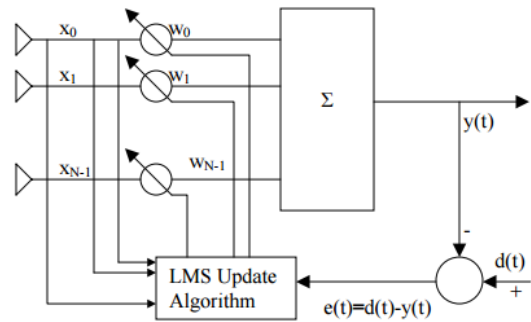
.

Figure 3: LMS adaptive beam-forming network.

3.1 Design of adaptive neuro-fuzzy inference controller

The best features of fuzzy systems and neural networks are integrated by adaptive neuro fuzzy inference system. Thus it has a potential of capturing benefits of both in a single frame network. ANFIS is a kind of artificial neural network that is based on Takagi-sugeno fuzzy inference system, which is having one input and one output.
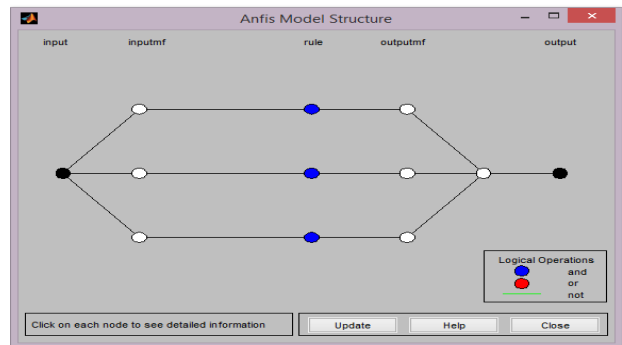

Figure 4: Optimized ANFIS architecture suggested by MATLAB/ANFIS editor.

The tool box function of ANFIS constructs data set fuzzy inference system(FIS) using given data set [8]. The membership functions are tuned by using back propagation algorithm. An initial data is generated from normal PI regulator in order to have idea of optimised ANFIS architecture. For future control the data is saved to workspace of MATLAB. In main MATLAB window ANFIS window is going to be opened by the command ANFIS editor. To generate an optimised ANFIS architecture as shown in figure 4. The data previously save in work space is loaded in the ANFIS command window.

The schematic of the proposed ANFIS architecture is given in figure 4. In ANFIS architecture the node functions of each layer are described.
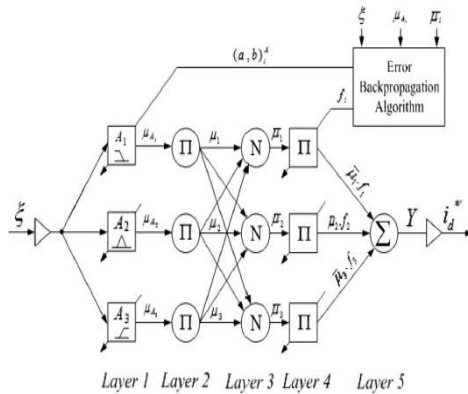
Figure 5: Schematic of the proposed ANFIS-based control architecture.

The neuro fuzzy controller is taking the error between reference dc-link voltage and actual dc-link voltage ($\xi=V_{dc}*-V_{dc}$) as input. The same error is used to tune the precondition and consequent parameters. The active power current component ($i_d *'$), is obtained by the control of DC link voltage, which is later modified to take in account of active current component injected from RES (i_{Ren}) [10-11]. In ANFIS architecture the node functions are as described below:

Layer 1: This layer is fuzzification layer here each node is represented by a square. The three membership functions are given to each input. In order to reduce the computation burden Trapezoidal and triangular membership functions are used as shown in Fig. 5 and the corresponding node equations are as given below:

$$\mu_{A1}(\varepsilon) = \begin{cases} 1 & \varepsilon \le b_1 \\ \frac{\varepsilon - a_1}{b_1 - a_1} & b_1 < \varepsilon < a_1 \\ 0 & \varepsilon \ge a_1 \end{cases} \qquad (6)$$

$$\mu_{A2}(\varepsilon) = \begin{cases} 1 - \frac{\varepsilon - a_1}{0.5b_2} & |\varepsilon - a_2| \le 0.5b_2 \\ 0 & |\varepsilon - a_2| \ge 0.5b_2 \end{cases} \qquad (7)$$

$$\mu_{A3}(\varepsilon) = \begin{cases} 0 & \varepsilon \le a_3 \\ \frac{\varepsilon - a_1}{b_3 - a_1} & a_3 < \varepsilon < b_3 \\ 1 & \varepsilon \ge b_3 \end{cases} \qquad (8)$$

(a_i, b_i) are values of parameters which changes the error according to the generated linguistic value of particular membership function. Here the parameters are referred as precondition parameters or as premise parameters .
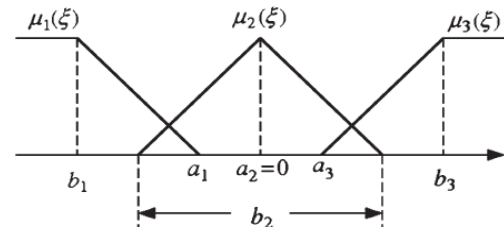
Figure 6: Fuzzy membership functions.

Layer 2: Each node in this layer is a circle labeled as Π. which multiplies the incoming signals and forwards it to next layer.

$$\mu_i = \mu_{Ai}(\varepsilon_1).\mu_{Bi}(\varepsilon_2) \ldots \ldots \text{ i= 1, 2, 3.} \qquad (9)$$

There is only one input in our case, so this layer is ignored and the third layer gets input whatever is the output of first layer. The firing strength of a rule is represented by the output of each node.

Layer 3: Each node is represented as circle in this layer. The normalized firing strength of each rule is calculated as given below:

$$\overline{\mu_i} = \frac{\mu_i}{\mu_1 + \mu_2 + \mu_3} \qquad . \qquad (10)$$

Layer 4: Every node in this layer is a node function

$$O_i = \overline{\mu_i}.f_i = \overline{\mu_i}\left(a_0^i + a_1^i \varepsilon\right) \text{ i=1,2,3} \qquad (11)$$

(a_0^i, a_1^i)are the parameters which are to be tuned as the function of input (ξ). Here the parameters are also referred as consequent parameters in this layer.

Layer 5: This layer is called as output layer which computes the output.

$$Y = \overline{\mu_1}.f_1 + \overline{\mu_2}.f_2 + \overline{\mu_3}.f_3 \qquad (12)$$

To obtain the active power current component (i_d*') the output from this layer is multiplied with normalizing factor.

IV. MATLAB/SIMULINK RESULTS

The PMSM-VSI drive system has been analyzed by this concept in MATLAB/simulation. The ANFIS&LMSA-DSC performance has been evaluated and the results are shown in this section.

In order to get the control behavior of PMSM drive system, different speed reference steps have been applied to the system. A negative *d* current must be injected Above the rated speed, to weaken the stator flux [13]. In some situations, the stator voltage tends to raise above the rated voltage of the drive and the speed cannot be increased anymore. Here the drawback is the reduction of the available torque since the current is partially used for flux weakening. Moreover, the field weakening can be further divided. For meeting the voltage limit above a certain velocity, a negative *d* current is also necessary at steady state.

The electric states stay on the MTPA trajectory for the first speed reference step is 0-1000rpm. 1000rpm is below rated speed and no field weakening is necessary. The second speed reference step is 1000 to 2000 rpm. The step can be seen as step from the standard operation region to the field weakening region. At 2000rpm, peak torque cannot be obtained any more since it would lead to a violation of the voltage limit. However, no *d* current injection is required for operation at 2000rpm without load torque. Thus, the third step is from 2000 to 3000 rpm. At 3000rpm, *d* current must be injected also without producing significant torque in order to fulfill the voltage limit.
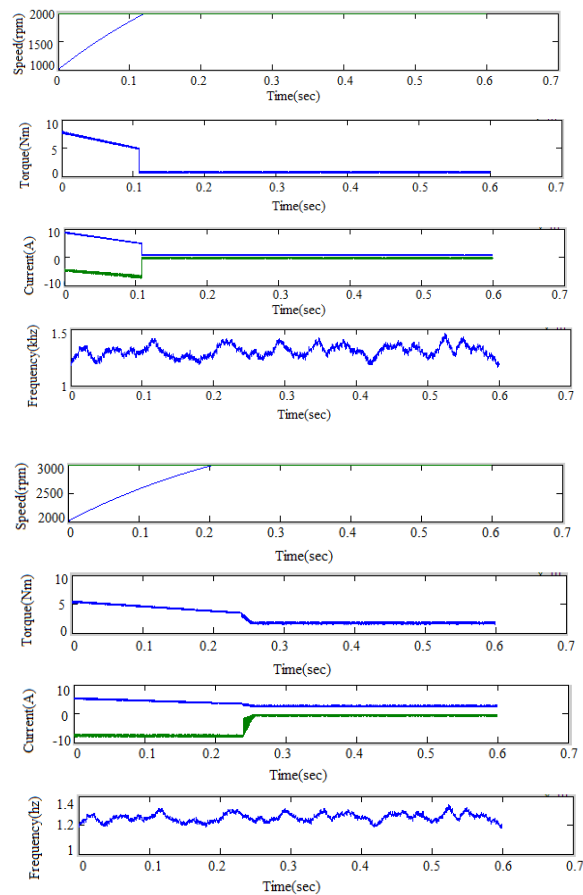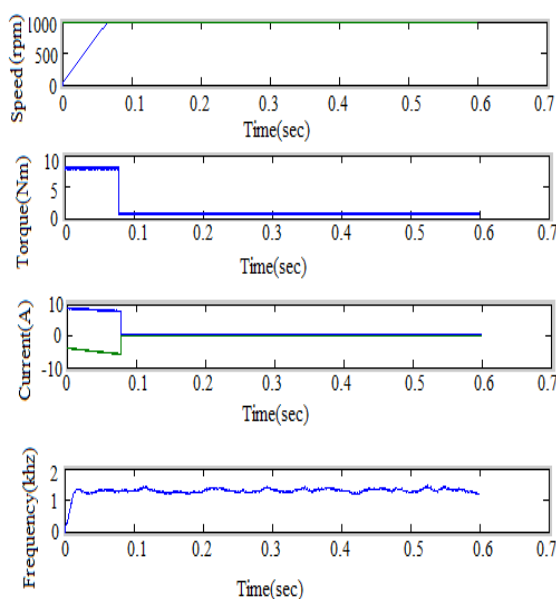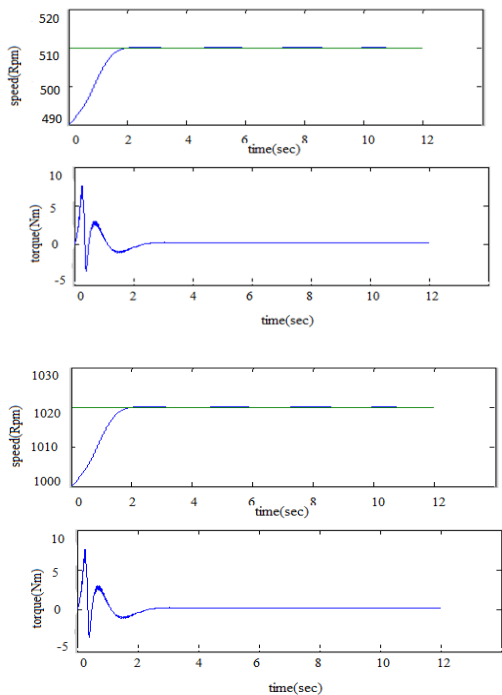

Figure 7: Simulation results: speed reference steps; from top:1000,2000,3000 rpm reference and measured speed, and electrical torque. Speeds below and above rated speed by MPC controller.

The simulation results are shown in Fig. 7. In this figure, the reference and measured speed are shown. Also, the electrical torque, the *dq* currents, and the switching frequency are shown.

The tracking component is dominant when the steps are applied. Until the speed error becomes small, a high torque is applied. The attraction region becomes important, when this happens. To maintain the speed, the lowest admissible current should be applied which permits. Even if no load torque is applied Electrical torque is still necessary to compensate the mechanical losses at steady state.

The speed control performance of the system is evaluated in this section. Small speed reference steps have been applied to the system. In order to avoid saturation of the system the steps are scaled, in first place the limitation of the torque, i.e. the currents.

Figure8: Simulation result: two speed reference steps without torque saturation (20rpm=0.6%); from top: reference and measured speed, and electrical torque by MPC controller.

it is difficult to find analytical performance, Since the system is nonlinear. It indexes like the high frequency cutoff (which corresponds to the bandwidth due to the low – pass behavior).

However in order to give an idea about performance, a Gaussian response H (w) = $e - \dfrac{w^2}{\sigma^2}$ can be assumed. Thus, the further called practical band width f_{bw} of the corresponding system can be approximated knowing the 10% - 90% rise time t_r using

$$f_{bw} = \frac{0.34}{t_r} \qquad (13)$$

The average raise times are about $t_r = 3\,\text{ms}$ and $t_r = 5\,\text{ms}$, for the step responses have been studied and they are shown in Figures. 6 and 7. The corresponding practical bandwidths are $f_{bw} = 113$ and 68 Hz in simulation. Due to the encoder, this produces a speed measurement with an overlaid discrete noise. In simulation, the effect has not been taken into account.

The load torque is the main disturbance, i.e,, tends to lead to prediction errors. Due to cost and reliability considerations, generally, it cannot be compensated since a measure must be avoided. The evaluation using the cost function and results in a speed offset are influenced by

potential error. Of course, such an offset should be avoided. Improvement comes along using the compensation.
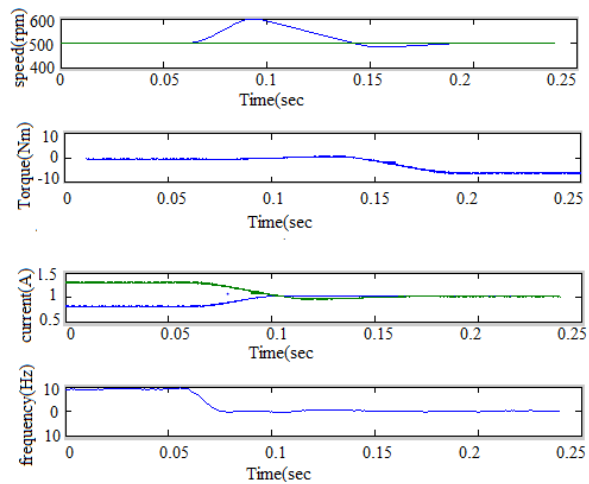
Figure 9: Simulation result: Load Torque step reference and measured speed electrical Torque dq currents and switching frequency by MPC controller.

By forcing the error between predicted and measured speed to zero, the disturbance is compensated. This implies that the offset in speed regulation is compensated. The concept is evaluated in simulation in Fig.8. A load torque step $T_l = 6\,N.m$ (about 80%) is applied at n = 500 r/min. the resulting speed variation is 110r/min (about 3.5%) before it gets compensated. In the figure 9, the reference and measured speed, the electrical torque, the dq currents, and the switching frequency are shown.
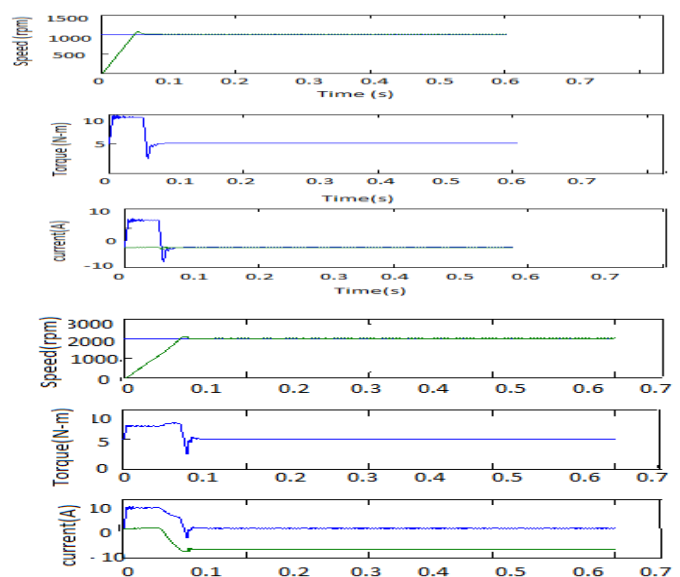
Figure 10:simulation result: speed reference step of speed, torque, current. Done by ANFIS controller for speeds 1000,2000 rpm.

Figure 10 gives the knowledge of reduced system dynamics that means increased system performance speed the settling time is very low in ANFIS and LMSA compared to actual model predictive controller.ANFIS is one of the best tradeoff between neural and fuzzy systems, providing: smoothness, due to the FC interpolation adaptability, due to the NN Back propagation. As compared to figure 7 and figure 10 the response of speed, torque and current has been settled earlier and reached steady state so we can say that ANFIS LMSA control is faster than MPC controller except computational complexity [12].
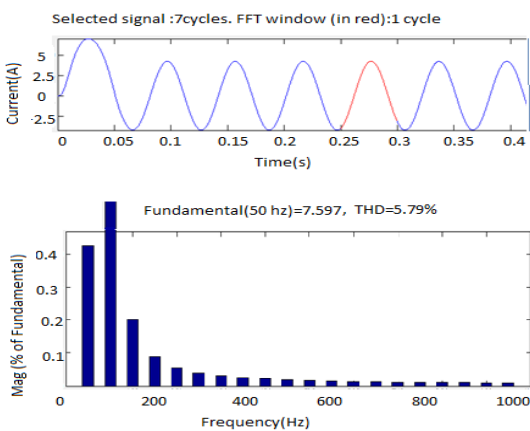

Figure 11: The current wave analyzed and the THD evaluated by MPC is 5.79%.
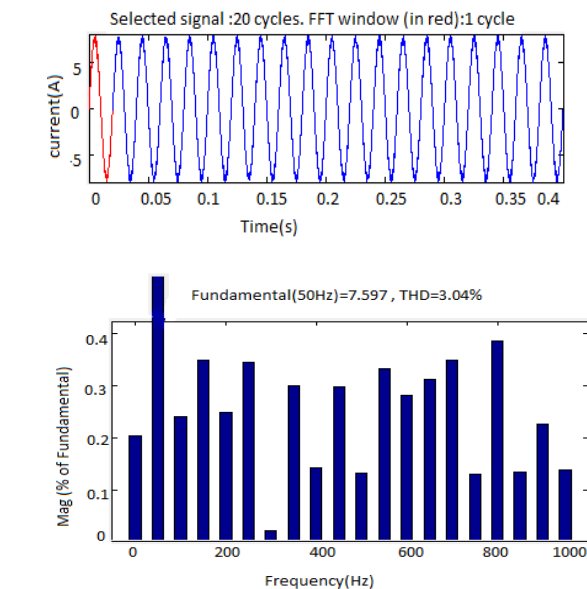

Figure.12: The Current wave analyzed and THD value evaluated by ANFIS 3.04%.

The response of the current, corresponding switching frequency is analyzed using FFT analysis in MATLAB and determined the THD as 3.04% for ANFIS-LMSA which is less compared to MPC analysis which has a value of THD 5.79%.

V. CONCLUSION

A speed controller has been successfully designed for the PMSM drive closed loop operation so that motor runs at the reference speed. The calculation of efficiency, average losses and measurement of voltages, currents is done by the simulation in each part of the system is possible. The PMSM drive has a detailed simulink model has been developed. By using the two current control schemes the operation above the rated speed and at the rated speed has been studied. Basically in such a system the inverter may be driven by ANFIS-LMSA controller. In working with analog and digital devices it is very flexible so that the simulation tools taken from different Simulink models. ANFIS and LMSA control is advantageous to MPC controller. If a higher switching frequency is acceptable, the THD can be reduced using a smaller sampling period, here getting a reduced THD value 3.04%.Table.1 shows Comparison Results.

Controller	THD value in % for current
MPC	5.79
ANFIS	3.04

Table 1: Comparison results of MPC and ANFIS

REFERENCES

[1]   Model Predictive Direct Speed Control with Finite Control Set of PMSM Drive Systems Matthias Preindl and Silverio Bolognani, *Member, IEEE*

[2]   Permanent magnet synchronous motor drive system for Mechatronics applications Adel El Shahat1,* & Hamed El Shewy2

[3]   predictive direct torque control with finite control set for PMSM drive systems." IEEE Trans. Ind. Inf., to be published.

[4]   M. Preindl and S. Bolognani, "Model Predictive direct torque control with finite control set for PMSM drive systems: Field weaking operation." IEEE Trans. Ind. Inf. To be published.

[5]   T. M. Jahns and V. Blasko, "Recent advances in power electronics technology for industrial and traction machine drives," Proc. IEEE, vol. 89, pp. 963–975, June 2001.

[6]   W.S. Levine, the control Handbook. Boca Raton: FL: CRC Press, 1996.

[7]   *The Fuzzy Logic Toolbox for use with MATLAB,* J.S.R. Jang and N. Gulley, Natick, MA: The MathWorks Inc., 1995.

[8]   "ANFIS: Adaptive-Network-Based Fuzzy Inference System", J.S.R. Jang, *IEEE Trans. Systems, Man, Cybernetics*, 23(5/6):665-685, 1993.

[9]   *Machine Learning, Neural and Statistical Classification* Michie, Spiegelhart& Taylor (Eds.), NY: Ellis Horwood 1994.

[10]   A DSC Approach to Robust Adaptive NN Tracking Control for Strict-Feedback Nonlinear Systems Tie-Shan Li, Dan Wang, Gang Feng, and Shao-Cheng Tong.

[11]   ANFIS: Adaptive-Network-Based Fuzzy Inference System Jyh-Shing Roger Jang.

[12]   A Nonlinear Control Method Based on ANFIS and Multiple Models for a Class of SISO Nonlinear Systems and Its Application Yajun Zhang, Tianyou Chai, and Hong Wang.

[13]   S.V. Emeljanov, Automatic control systems with variable structure, R. Oldenbourg – Verlag: Munich Germany, 1969.

[14]   B. K. Bose, "Power electronics and motion control-Technology status and recent trends," IEEE Trans. Ind. Applicat, vol. 29, pp. 902–909, Sept. /Oct., 1993.